Guest selectivity of [Ni_2] supramolecular helicates

Manuel Imperato,[a,b,c] Alessio Nicolini,[a] Jordi Ribas-Ariño,[d] Michał Antkowiak,[c,e] Olivier Roubeau,[f] Andrea Cornia,[a,*] Valentin Novikov,[c,g] Leoní A. Barrios[c,g,*] and Guillem Aromí.[c,g,*]

Supporting Information

Synthesis

Ligand L was prepared according to a modified published procedure.[1] Below is the full procedure employed here.

3,3'-(1,3-phenylene)bis(1-(pyridin-2-yl)propane-1,3-dione) (**L1**)

In a 50 mL Schlenk flask, NaH (60% oil dispersion, 2.0086 g, 50.22 mmol) was suspended in *n*-hexane (20 mL) and stirred for 10 minutes under N_2 atmosphere, and then the solvent was removed with a Pasteur pipette to separate the mineral oil. This procedure was repeated after addition of further *n*-hexane (20 mL) and then dry THF (35 mL) was added to the resulting white solid. In a separate 250 mL Schlenk flask, 1,3-diacetylbenzene (2.0023 g, 12.35 mmol) was dissolved under N_2 in dry THF (120 mL) and then, the whitish THF suspension of NaH was added to it dropwise. While the reaction mixture turned yellow, the stirring was maintained for 15 minutes at room temperature. 2-Ethylpicolinate (3.4 mL, 25.17 mmol) was added dropwise to the reaction mixture, which then turned green. The reaction was then heated under N_2 to 60 °C, in a careful manner to avoid the abrupt evolution of hydrogen, and then gently brought to reflux causing a sudden change to brownish colour. After 18 h of reflux, an orange-brownish suspension was obtained that was then allowed to cool to room temperature. EtOH (5 mL) was then added to quench the unreacted NaH and the precipitate was collected by filtration through a fritted glass funnel (porosity G3). The resulting brown solid was then suspended in H_2O (150 mL) and the pH was adjusted to 3 using HCl 37%, producing a change of color to yellow and the precipitation of a beige solid; then the mixture was left for 30 minutes under stirring. The beige solid was collected by filtration (fritted glass funnel, porosity G3) and thoroughly washed with H_2O until the filtrate was colorless. The very sticky solid so obtained was then washed with Et_2O, dried under vacuum, dissolved in CH_2Cl_2 (150 mL) and stirred for 20 minutes, giving a biphasic system. The red organic phase was then separated and dried over Na_2SO_4. The desiccant was removed by filtration and the organic solution was evaporated to dryness, to give a grey solid (2.4912 g, 54.2%). The ^{1}H NMR spectrum ($CDCl_3$, 400.13 MHz, 298 K) is consistent with that reported in the quoted paper .

1,3-bis(3-(pyridin-2-yl)-1*H*-pyrazol-5-yl)benzene (L)

In a 250 mL round bottom flask, L1 (1.5014 g, 4.03 mmol) was suspended in MeOH (100 mL). To this yellow-brownish suspension, hydrazine monohydrate (64% in H_2O, 3.0 mL, 39.6 mmol) was added dropwise, and the mixture was heated under reflux overnight. During the initial 30 minutes of reaction the system first turned red and then the precipitation of a white solid was observed. Upon completion of the reaction, the resulting whitish-milky suspension was allowed to cool to room temperature and the white

[1] M. Darawsheh, L. A. Barrios, O. Roubeau, S. J. Teat, G. Aromí, *Chem., Eur. J.* **2016**, *22*, 8635-8645.

precipitate was collected by filtration through a fritted glass funnel (porosity G3) and washed with MeOH (10 mL). The solid was then dried under vacuum to give a white powder (988 mg, 67.2%). An additional crop was collected evaporating the filtrate to dryness, suspending the resulting solid into 50 mL of H_2O and filtering the mixture (fritted glass funnel, porosity G3). The solid obtained was then washed with $CHCl_3$ and dried under vacuum to give a white powder (additional 19.2%, 282 mg). The ^1H NMR spectrum (DMSO-d_6, 400.13 MHz, 298 K) is consistent with that reported in the quoted paper.

Cl@[Ni$_2$L$_3$]Cl(BF$_4$)$_2$ (1). A whitish suspension of L (125.2 mg, 0.344 mmol) in MeOH (50 mL) was added dropwise to a stirred slightly green solution of $NiCl_2 \cdot 6H_2O$ (54.8 mg, 0.231 mmol) in MeOH (25 mL). A pink suspension formed, which was stirred for 45 minutes, giving a pink transparent solution. This solution was filtered, and the filtrate mixed with a solution of $TBABF_4$ (150.7 mg, 0.460 mmol) in MeOH (10 mL). The resulting solution was layered with Et_2O. Lilac blocks formed after approximately two weeks (yield 15.1%). EA (%) calcd. for **1**·1.65MeOH·4.8H_2O (found): C 50.96 (50.57), H 4.06 (3.66), N 15.81 (15.31). ESI-MS (MeCN, positive ion mode): *m*/*z* = 414.42, $(Cl@[Ni_2L_3])^{3+}$; 621.13, $(Cl@[Ni_2L_3]-H^+)^{2+}$; 665.14, $(Cl@[Ni_2L_3]BF_4)^{2+}$.

Br@[Ni$_2$L$_3$]Br$_2$(BF$_4$) (2). A whitish suspension of L (126.1 mg, 0.346 mmol) in MeOH (50 mL) was added dropwise to a stirred colorless solution of $Ni(BF_4)_2 \cdot 6H_2O$ (78.6 mg, 0.231 mmol) in MeOH (25 mL). A pink suspension formed, which was stirred for 45 minutes, giving a pink transparent solution. This solution was filtered, and the filtrate mixed with a solution of TBABr (147.9 mg, 0.459 mmol) in MeOH (10 mL). The resulting solution was layered with Et_2O. Lilac blocks of formed after approximately two weeks (39.5 mg, 15.5%). EA (%) calcd. for **2**·1.3MeOH·5H_2O (found): C 48.44 (48.56), H 3.82 (3.40), N 15.12 (14.69). ESI-MS (MeCN, positive ion mode): *m*/*z* = 429.07 $(Br@[Ni_2L_3])^{3+}$; 643.11, $(Br@[Ni_2L_3]-H^+)^{2+}$; 687.11, $(Br@[Ni_2L_3]BF_4)^{2+}$.

Single Crystal X-Ray Diffraction (SCXRD)

Data for compounds **1**·3MeOH·4H_2O and **2**·10MeOH·5H_2O (hereafter referred to as **1** and **2** for simplicity) were obtained at 100 K on the BL13-XALOC beamline of the ALBA synchrotron (λ = 0.72932 Å),[2] on a lilac blocks of dimensions 0.150 x 0.050 x 0.050 mm^3 and 0.100 x 0.080 x 0.080 mm^3 respectively. Data reduction and absorption corrections were performed with SAINT and SADABS, respectively.[3] The structures were solved by intrinsic phasing with SHELXT[4] and refined by full-matrix least-squares on F^2 with SHELXL.[5] In both structures, a significant portion of the lattice methanol molecules were too diffuse to be refined, and the corresponding voids were analyzed and taken into account using SQUEEZE,[6] resulting in 2 and 9 diffuse methanol molecules per formula unit for **1** and **2**, respectively.

All details can be found in CCDC 2343092 (**1**) and 2343093 (**2**) that contain the supplementary crystallographic data for this paper. These data can be obtained free of charge from The Cambridge Crystallographic Data Center via https://www.ccdc.cam.ac.uk/structures/. Crystallographic and refinement parameters are summarized in Table S1. The results of continuous shape measures are presented in Table S2 while selected interatomic distances and angles are given in Tables S3 and S4.

[2] J. Juanhuix, F. Gil-Ortiz, G. Cuní, C. Colldelram, J. Nicolás, J. Lidón, E. Boter, C. Ruget, S. Ferrer and J. Benach, *J. Synchrotron Radiat.*, 2014, **21** , 679-689
[3] G. M. Sheldrick, 2012, *SAINT and SADABS*, Bruker AXS Inc., Madison, Wisconsin, USA.
[4] G. M. Sheldrick, *Acta Cryst. A*, 2015, **71**, 3-8
[5] G. M. Sheldrick, *Acta Cryst. C*, 2015, **71**, 3-8
[6] A. L. Spek, *Acta Cryst. C*, 2015, **71**, 9-18

Table S1. Crystallographic and refinement parameters for the structures of compounds **1** and **2**.

	1	**2**
Formula	$C_{66}H_{48}N_{18}Ni_2$, 2(BF_4), 2 (Cl), 3(CH_4O), 4(H_2O)	$C_{66}H_{48}N_{18}Ni_2$, BF_4, 3(Br), 10(CH_4O), 5(H_2O)
FW (g mol^{-1})	1623.35	1947.66
T (K)	100	100
Wavelength (Å)	0.72932	0.72932
Crystal system	tetragonal	tetragonal
Space group	*I*–4	*I*–4
a (Å)	29.264(4)	30.0486(13)
b (Å)	29.264(4)	30.0486(13)
c (Å)	17.389(3)	19.3054(9)
α (°)	90	90
β (°)	90	90
γ (°)	90	90
V (Å^3)	14892(5)	17431.2(17)
Z	8	8
ρ_{calcd} (g cm^{-3})	1.448	1.485
μ (mm^{-1})	0.685	2.288
Independent reflections (R_{int})	10667 (0.0378)	18367 (0.0402)
parameters / restraints	993 / 251	930 / 52
Flack parameter	0.043(5)	0.111(4)
Goodness-of-fit	1.058	1.054
Final R1 / wR2 [I>2σ(I)]	0.0882 / 0.2311	0.0991 / 0.2786
Final R1 / wR2 [all data]	0.1027 / 0.2539	0.1068 / 0.2911
largest diff. peak / hole (e Å^3)	1.535 / –0.474	1.864 / –1.668

Table S2. Distances to the ideal octahedron (O_h) or trigonal prism (D_{3h}) of the Ni ions of compounds 1 and 2 obtained with symmetry measures using the program SHAPE.[7]

	Compound **1**		Compound **2**	
	Ni1	Ni2	Ni1	Ni2
OC-6 (O_h)	1.597	1.354	1.363	1.525
TPR-6 (D_{3h})	11.226	13.017	12.319	11.447

[7] Alvarez, S.; Avnir, D.; Llunell, M.; Pinsky, M. Continuous symmetry maps and shape classification. The case of six-coordinated metal compounds. *New J. Chem.* **2002**, *26* (8), 996-1009, 10.1039/B200641N. DOI: 10.1039/B200641N.

Table S3. Selected interatomic distances [Å] and angles [°] in **1** at 100 K.

Ni1–N1	2.120(10)	Ni2–N12	2.139(11)	Ni2···Cl2B	4.889(14)
Ni1–N2	2.061(10)	Ni2–N17	2.060(10)	N3H··· Cl1	3.391[a]
Ni1–N7	2.094(11)	Ni2–N18	2.083(12)	N4H··· Cl1	3.342[a]
Ni1–N8	2.088(11)	Ni1···Ni2	9.663(3)	N9H··· Cl1	2.485[a]
Ni1–N13	2.176(10)	Ni1···Cl1	4.988(4)	N10H··· Cl1	2.586[a]
Ni1–N14	2.071(10)	Ni2···Cl1	4.692(4)	N15H··· Cl1	3.232[a]
Ni2–N5	2.095(12)	Ni1···Cl2A	5.007(10)	N16H··· Cl1	2.684[a]
Ni2–N6	2.130(10)	Ni2···Cl2B	7.346(16)	Ni1–Cl1–Ni2	173.27(8)
Ni2–N11	2.093(13)	Ni2···Cl2A	7.109(10)		

[a] These distances are provided without an estimated standard deviation because they involve hydrogen atoms placed in geometrically idealized positions and refined with a riding model.

Table S4. Selected interatomic distances [Å] and angles [°] in **2** at 100 K.

Ni1–N1	2.130(8)	Ni2–N17	2.095(8)	Ni2···Br3A	4.896(5)
Ni1–N2	2.078(8)	Ni2–N18	2.142(9)	Ni2···Br3B	7.169(7)
Ni1–N7	2.100(9)	Ni1···Ni2	9.7529(15)	Ni2···Br3C	5.527(11)
Ni1–N8	2.078(8)	Ni1···Br1	4.9166(18)	N3H···Br1	2.947[a]
Ni1–N13	2.127(8)	Ni2···Br1	4.8366(18)	N4H···Br1	2.799[a]
Ni1–N14	2.092(8)	Ni1···Br2	5.1579(18)	N9H···Br1	2.932[a]
Ni2–N5	2.095(9)	Ni2···Br2	7.343(2)	N10H···Br1	2.061[a]
Ni2–N6	2.120(9)	Ni1···Br3A	7.617(6)	N15H···Br1	2.911[a]
Ni2–N11	2.086(8)	Ni1···Br3B	4.882(4)	N16H···Br1	2.820[a]
Ni2–N12	2.129(8)	Ni1···Br3C	5.349(11)	Ni1–Br1–Ni2	179.06(4)

[a] These distances are provided without an estimated standard deviation because they involve hydrogen atoms placed in geometrically idealized positions and refined with a riding model.

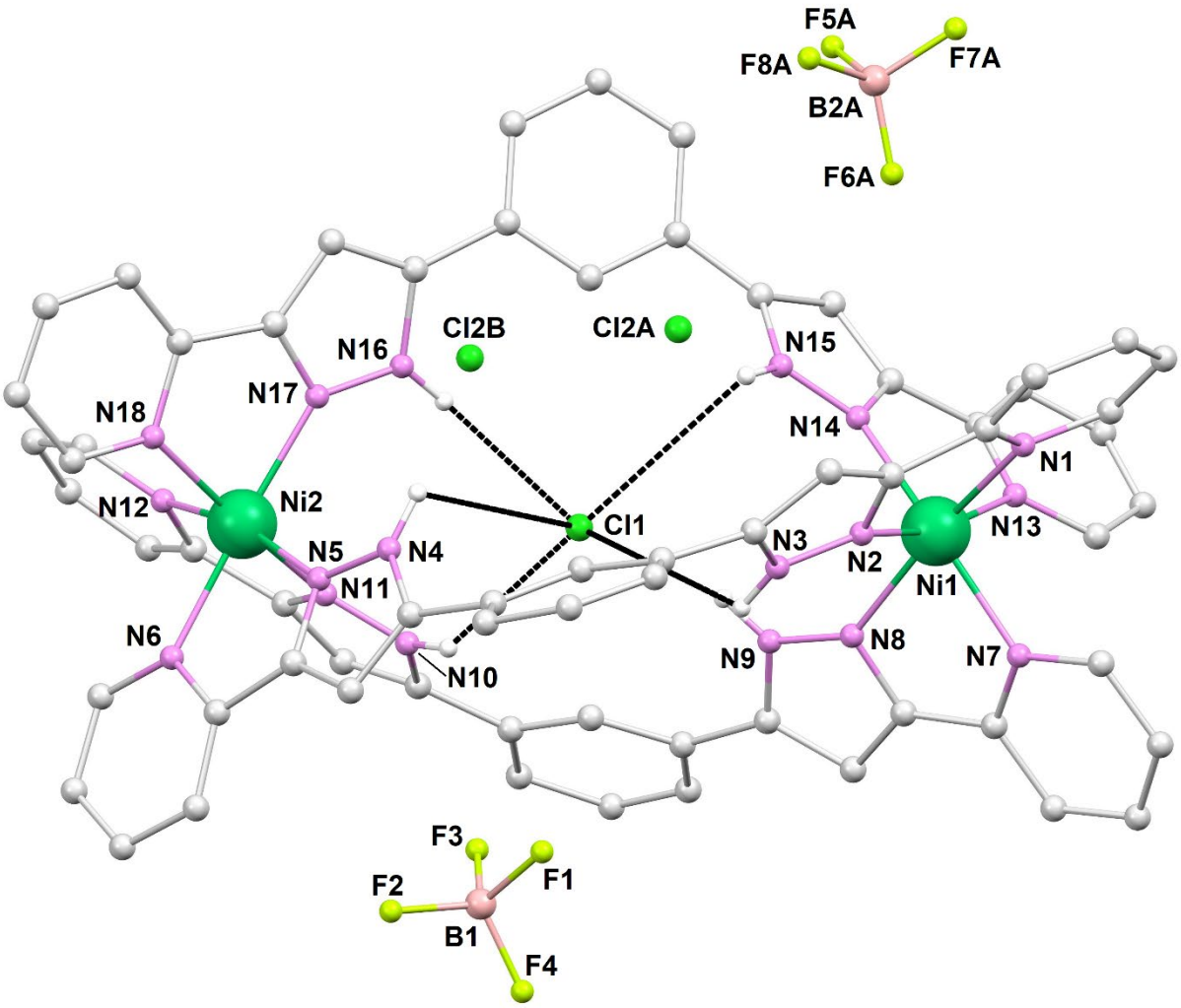

Figure S1. Representation of the salt Cl@[Ni_2L_3]Cl(BF_4)$_2$ (**1**) with heteroatoms labelled. Both disordered positions of Cl2 are shown, while only one of the positions of the disordered BF_4^- (A) anion is included. Only H atoms from N−H groups are shown. H-bonds are depicted using dashed lines.

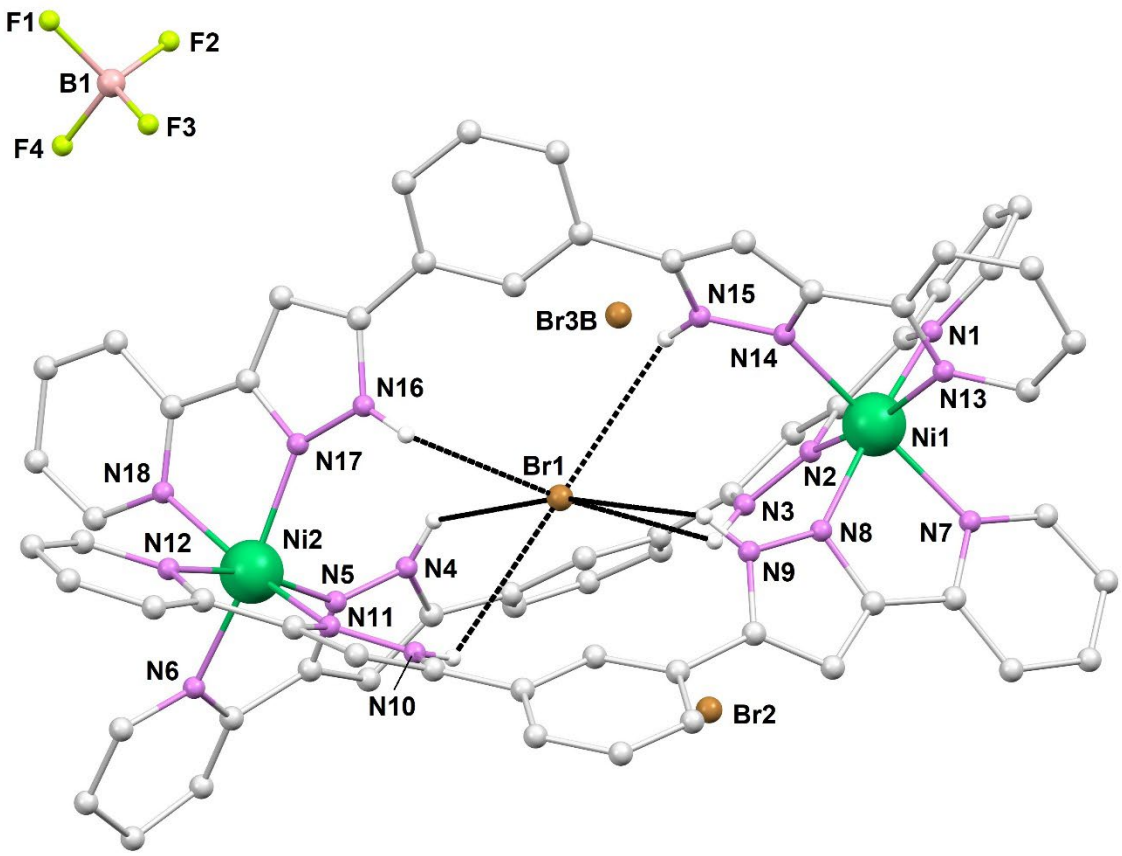

Figure S2. Representation of the salt Br@[Ni_2L_3]Br_2(BF_4) (**2**) with heteroatoms labelled. Only one of the three disordered positions of Br3 is shown. Only H atoms from N−H groups are shown. H-bonds are depicted using dashed lines.

Electrospray ionization mass spectrometry (ESI-MS)

Positive ion ESI-MS experiments were conducted by direct infusion of MeCN solutions on a Q Exactive Hybrid Quadrupole-Orbitrap Mass Spectrometer (Thermo Scientific) installed at the Centro Interdipartimentale Grandi Strumenti (CIGS) of the University of Modena and Reggio Emilia. Crystals of **1** and **2** were dissolved in MeCN to give $7.70 \cdot 10^{-5}$ and $8.00 \cdot 10^{-5}$ M solutions, respectively, which were treated with appropriate volumes of a CD_3CN solution of TBABr (0.096 M) and TBACl (0.104 M), respectively. No precipitation was observed in these conditions.

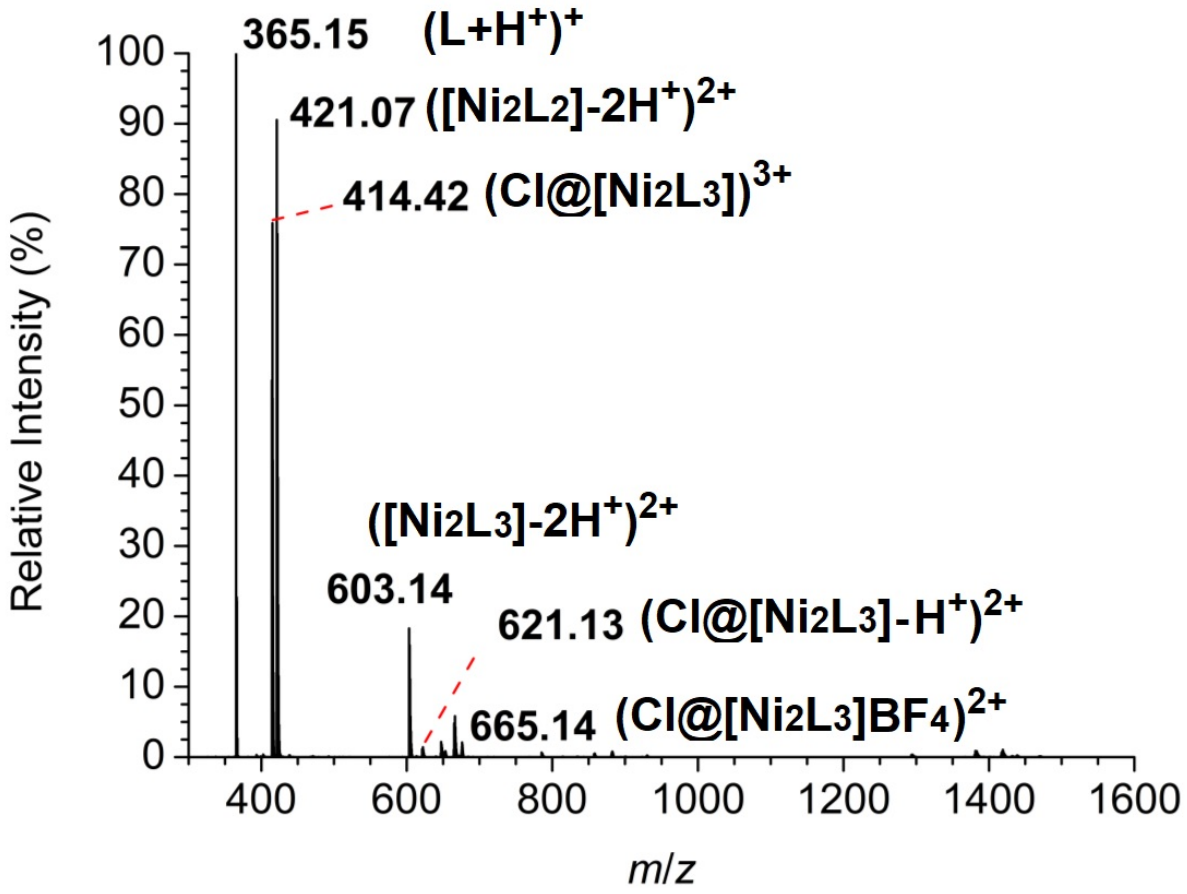

Figure S3. ESI-MS spectrum of **1** (direct infusion, MeCN, positive ion mode) with all the important peaks assigned.

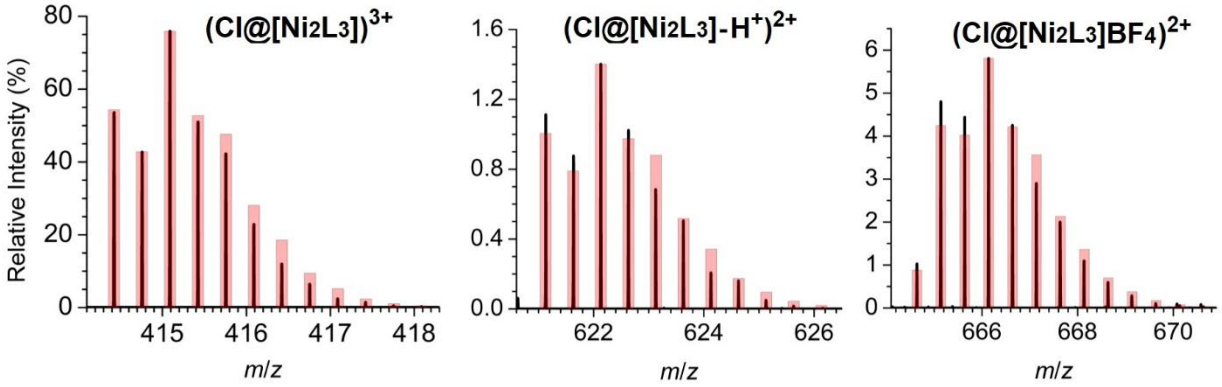

Figure S4. Detail of the experimental (black lines) and simulated (red columns) isotopic patterns of the peaks at *m*/*z* = 414.42 $(Cl@[Ni_2L_3])^{3+}$, 621.13 $(Cl@[Ni_2L_3]-H^+)^{2+}$ and 665.14 $(Cl@[Ni_2L_3]BF_4)^{2+}$.

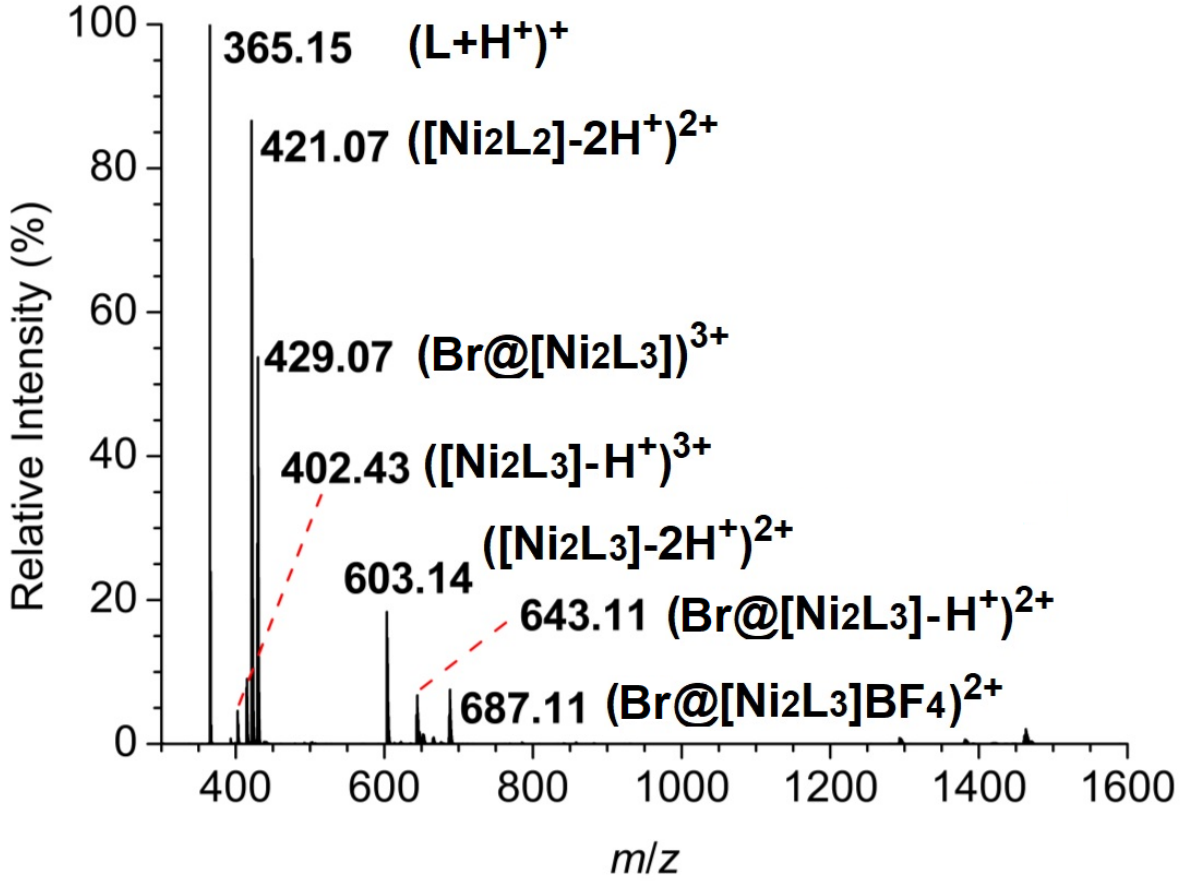

Figure S5. ESI-MS spectrum of **2** (direct infusion, MeCN, positive ion mode) with all the important peaks assigned.

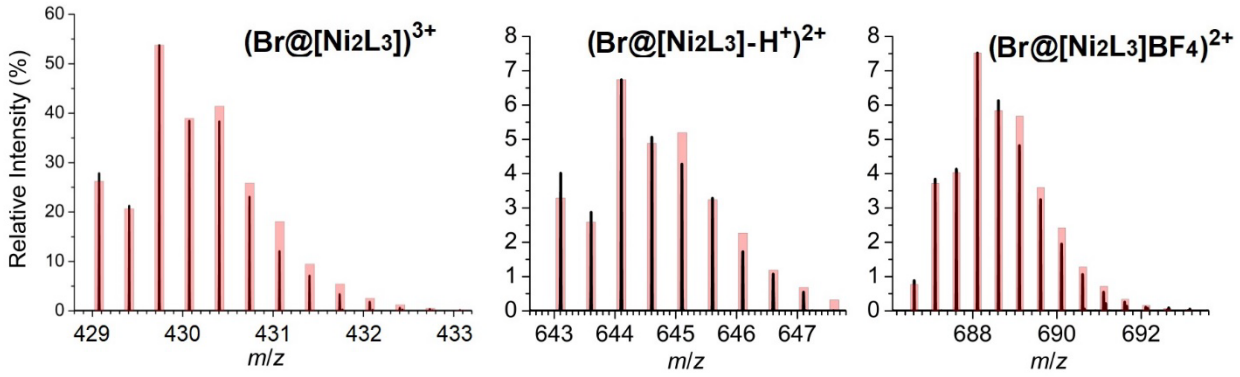

Figure S6. Detail of the experimental (black lines) and simulated (red columns) isotopic patterns of the peaks at *m*/*z* = 429.07 $(Br@[Ni_2L_3])^{3+}$, 643.11 $(Br@[Ni_2L_3]-H^+)^{2+}$ and 687.11 $(Br@[Ni_2L_3]BF_4)^{2+}$.

NMR Spectroscopy

NMR spectroscopy measurements were conducted on solutions in CD_3CN with a Bruker Avance 500 and Avance 300 FT-spectrometers (500.2 MHz and 300.1 MHz ^1H frequency, respectively) at the CCiTUB from the Universitat de Barcelona or with a Brucker Avance 400 FT spectrometer installed at the Centro Interdipartimentale Grandi Strumenti (CIGS) of the University of Modena and Reggio Emilia (operating at 400.13, 39.20, and 100.25 MHz for ^1H, ^{35}Cl, and ^{79}Br, respectively). All the experiments in Modena were conducted using 5 mm airtight Young-valved NMR tubes from Norell, to prevent a large entry of water and/or dioxygen over time. Spectra were analyzed using TopSpin (version 4.3.0).[8] ^1H spectra were calibrated setting the residual proton signal of the solvent at 1.94 ppm.[9] ^{35}Cl and ^{79}Br spectra were referenced to a 0.2 M D_2O solution of NaCl and NaBr, respectively. Crystals of **1** and **2** were dissolved in CD_3CN to give $5.5 \cdot 10^{-4}$ and $4.2 \cdot 10^{-4}$ M solutions, respectively, which were treated with appropriate volumes of a CD_3CN solution of TBABr (0.096 M) and TBACl (0.104 M), respectively.

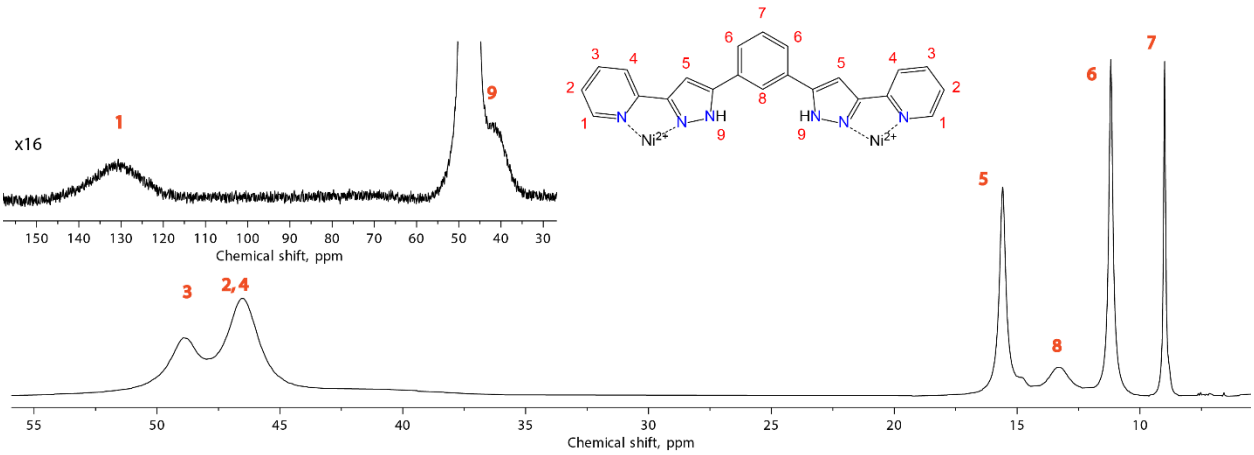

Figure S7. ^1H NMR spectrum (500 MHz, 298 K) of solution of compound **2** in CD_3CN with signal assignments.

[8] Bruker AXS Inc. TopSpin 4.3.0. Madison, Wisconsin, USA 2023.
[9] Fulmer, G. R.; Miller, A. J. M.; Sherden, N. H.; Gottlieb, H. E.; Nudelman, A.; Stoltz, B. M.; Bercaw, J. E.; Goldberg, K. I. NMR Chemical Shifts of Trace Impurities: Common Laboratory Solvents, Organics, and Gases in Deuterated Solvents Relevant to the Organometallic Chemist. Organometallics 2010, 29 (9), 2176–2179. https://doi.org/10.1021/om100106e.

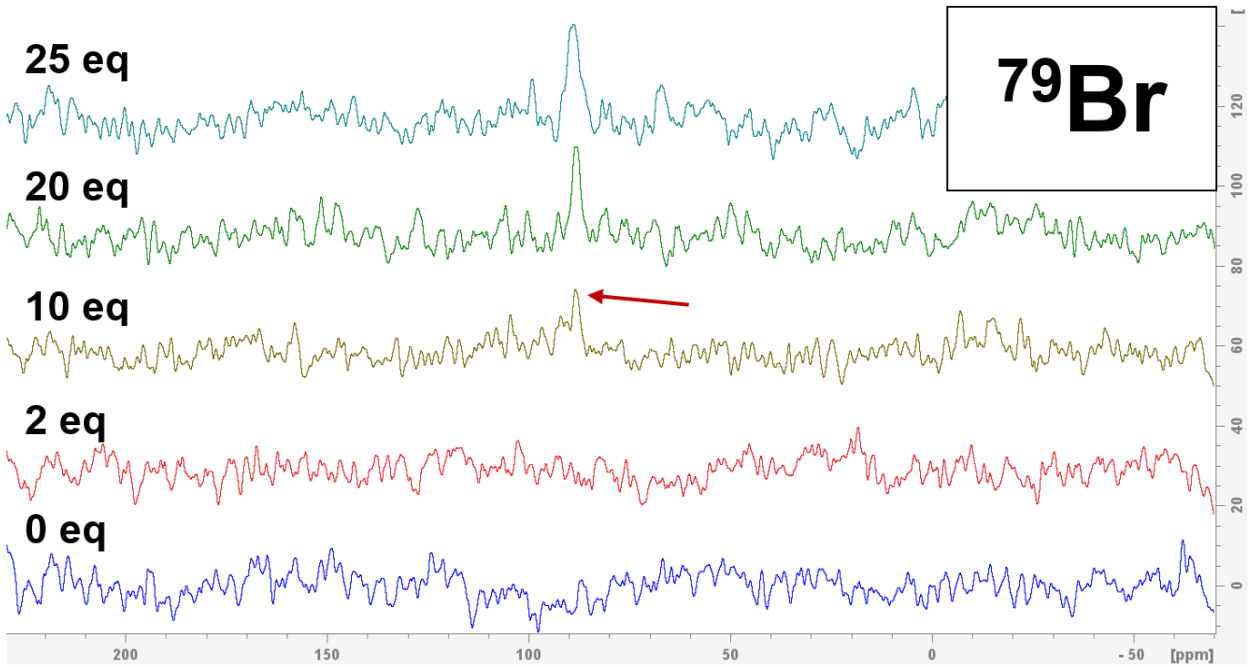

Figure S8. ^{79}Br NMR spectrum (100.25 MHz, 298 K) of a CD_3CN solution of compound **2** during the titration with TBACl, whose total added amounts are reported on the left. The red arrow indicates the barely visible signal of free Br^- ions after addition of 10 eq of titrant. Processing parameters: SI = TD, LB = 100 Hz.

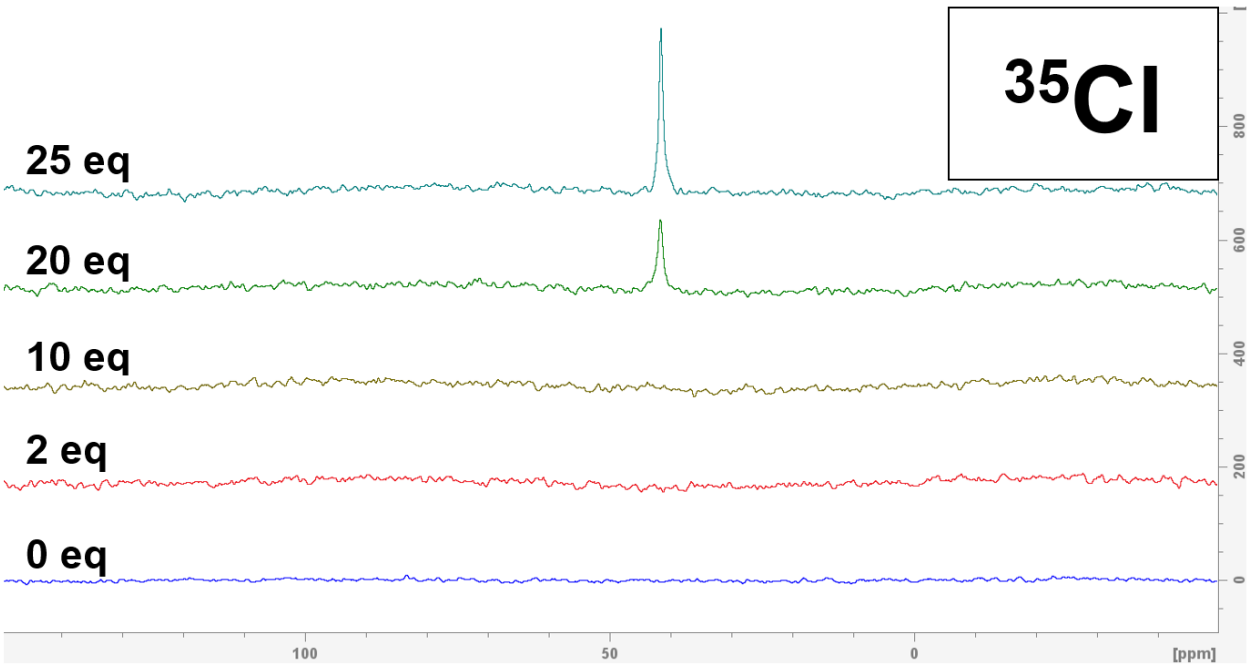

Figure S9. ^{35}Cl NMR spectrum (39.20 MHz, 298 K) of a CD_3CN solution of compound **2** during the titration with TBACl, whose total added amounts are reported on the left. Processing parameters: SI = TD, LB = 20 Hz.

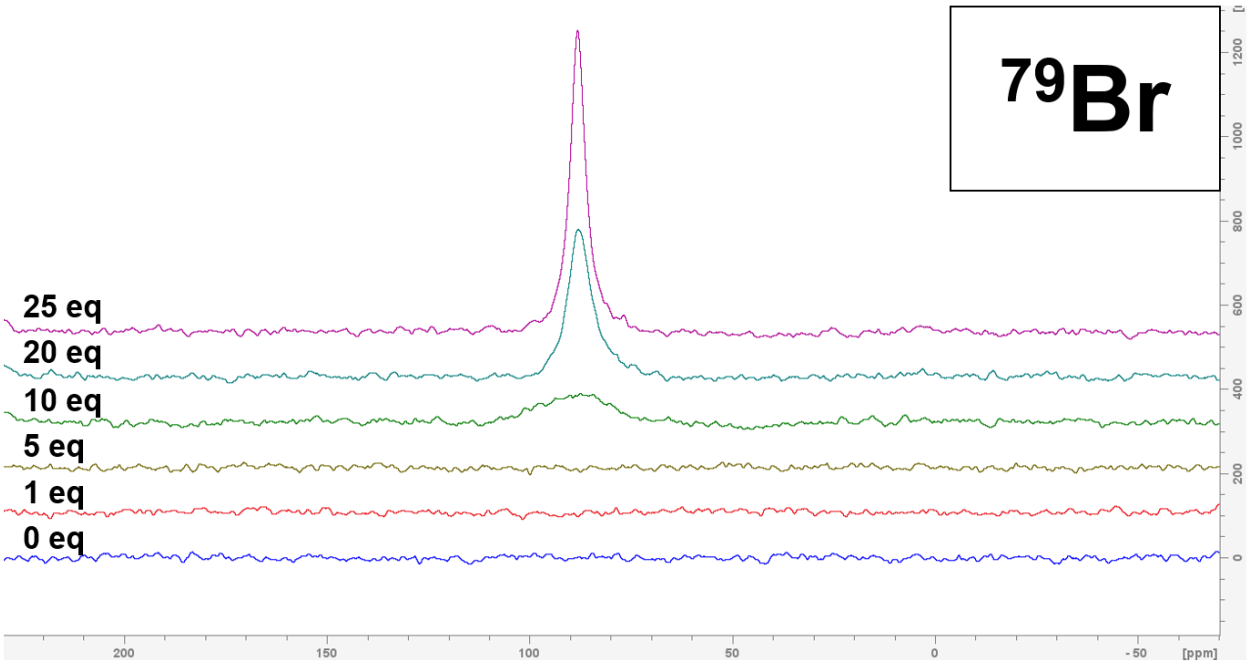

Figure S10. ^{79}Br NMR spectrum (100.25 MHz, 298 K) of a CD_3CN solution of compound **1** during the titration with TBABr, whose total added amounts are reported on the left. Processing parameters: SI = TD, LB = 100 Hz.

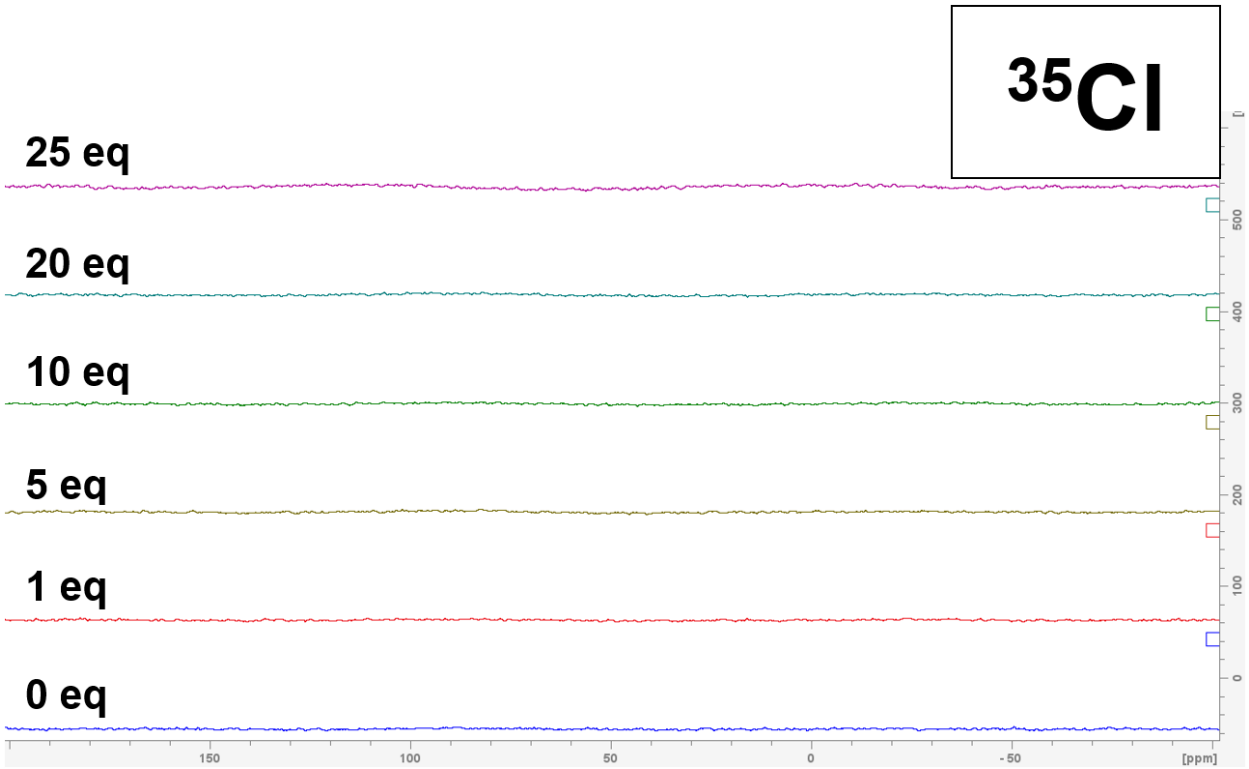

Figure S11. ^{35}Cl NMR spectrum (39.20 MHz, 298 K) of a CD_3CN solution of compound **1** during the titration with TBABr, whose total added amounts are reported on the left. Processing parameters: SI = TD, LB = 20 Hz.

DFT Calculations

The reaction energy associated with the process in Eq. S1 was evaluated after fully optimizing the geometry of reactants and products. These structural optimizations were carried out using density functional theory (DFT) based calculations employing the PBE[10] exchange-correlation functional in its spin unrestricted form and a def2-SVP[11] basis set using the Gaussian 16 code.[12] In all the calculations, the DFT-D3(BJ) semi-empirical dispersion potential introduced by Grimme[13] was added to the conventional Kohn–Sham energy for a proper description of the van der Waals interactions. Calculations in acetonitrile were performed using the polarizable continuum model.[14]

$$(Br@[Ni_2L_3])^{3+} + Cl^- \rightarrow (Cl@[Ni_2L_3])^{3+} + Br^- \qquad \text{(Eq. S1)}$$

Evaluation of the strength of the X$^-$ ⋯ N-H hydrogen bonds

The strength of the X$^-$⋯N−H hydrogen bonds was assessed by computing the interaction energy of a $[Ni(L_{cut})_3]^{2+}$ complex and the halide ion (Cl^- or Br^-), where L_{cut} is the relevant fragment of the ligand L (Figure 12). The interaction energy (E_{int}) was evaluated through:

$$E_{int} = E([Ni(L_{cut})_3]^{2+}\cdots X^-) - E([Ni(L_{cut})_3]^{2+}) - E(X^-)$$

where $E([Ni(L_{cut})_3]^{2+}\cdots X^-)$ is the electronic energy of the fully relaxed $([Ni(L_{cut})_3]^{2+}\cdots X^-)$ entity, $E([(L_{cut})_3]^{2+})$ is the electronic energy of the fully relaxed $[Ni(L_{cut})_3]^{2+}$ complex, and $E(X^-)$ is the electronic energy of the halide ion. In the $([Ni(L_{cut})_3]^{2+}\cdots X^-)$ entity, the halide ion establishes a hydrogen bond with every pyrazolyl moiety of the complex. Therefore, the halide ion forms three hydrogen bonds. According to the DFT calculations, the E_{int} value for Cl^- is 19.8 kcal mol^{-1} more negative than for Br^-, thus rendering the interaction stronger.

---

[10] J.P. Perdew, K. Burke, M. Ernzerhof, *Phys. Rev. Lett*. 1996, **77**, 3865–3868.
[11] F. Weigend, R. Ahlrichs, *Phys. Chem. Chem. Phys*., 2005, **7**, 3297-3305.
[12] Gaussian 16, Revision B.01, M. J. Frisch, G. W. Trucks, H. B. Schlegel, G. E. Scuseria, M. A. Robb, J. R. Cheeseman, G. Scalmani, V. Barone, G. A. Petersson, H. Nakatsuji, X. Li, M. Caricato, A. V. Marenich, J. Bloino, B. G. Janesko, R. Gomperts, B. Mennucci, H. P. Hratchian, J. V. Ortiz, A. F. Izmaylov, J. L. Sonnenberg, D. Williams-Young, F. Ding, F. Lipparini, F. Egidi, J. Goings, B. Peng, A. Petrone, T. Henderson, D. Ranasinghe, V. G. Zakrzewski, J. Gao, N. Rega, G. Zheng, W. Liang, M. Hada, M. Ehara, K. Toyota, R. Fukuda, J. Hasegawa, M. Ishida, T. Nakajima, Y. Honda, O. Kitao, H. Nakai, T. Vreven, K. Throssell, J. A. Montgomery, Jr., J. E. Peralta, F. Ogliaro, M. J. Bearpark, J. J. Heyd, E. N. Brothers, K. N. Kudin, V. N. Staroverov, T. A. Keith, R. Kobayashi, J. Normand, K. Raghavachari, A. P. Rendell, J. C. Burant, S. S. Iyengar, J. Tomasi, M. Cossi, J. M. Millam, M. Klene, C. Adamo, R. Cammi, J. W. Ochterski, R. L. Martin, K. Morokuma, O. Farkas, J. B. Foresman, and D. J. Fox, Gaussian, Inc., Wallingford CT, 2016.
[13] S. Grimme, S. Ehrlich and L. Goerigk, *J. Comp. Chem*. 2011, **32**, 1456-65.
[14] J. Tomasi, B. Mennucci, and R. Cammi, *Chem. Rev.*, 2005, **105**, 2999-3093.

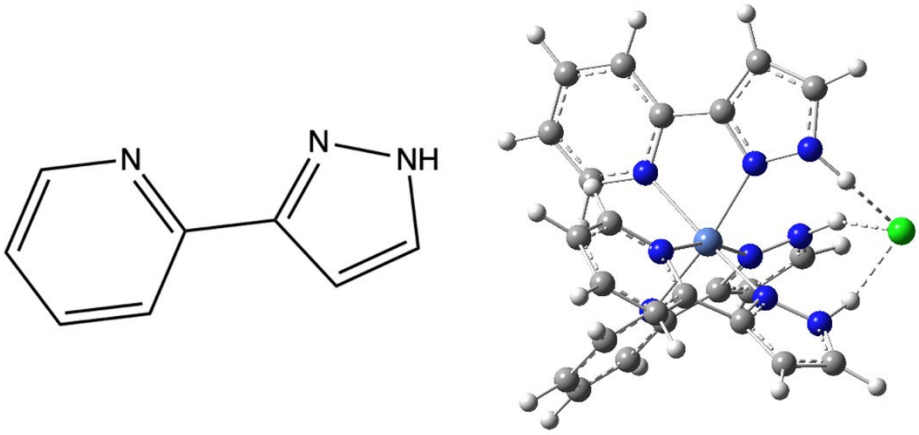

Figure S12. (Left) Structure of the ligand used to evaluate the strength of the $X^{-}\cdots$N-H hydrogen bonds. (Right) Representation of the optimized structure of the $[NiL_{cut}]^{2+}\cdots Cl^{-}$ entity.

Magnetic Properties

Magnetic measurements were performed using either a Quantum Design SQUID evercool MXL7 magnetometer at the "Unitat de Mesures Magnètiques" of the Universitat de Barcelona or a Quantum Design MPMS3 SQUID magnetometer hosted by the Physical Measurements Unit of the Servicio General de Apoyo a la Investigación-SAI, Universidad de Zaragoza. Samples were mounted within gelatine capsules hosted in plastic straw. Variable temperature *dc* data were collected with an applied field of 5000 Oe, in settle mode.

The approximation used for modeling the magnetic behavior of both compounds is expressed with the following Hamiltonian:

$$\hat{H} = D\left(\hat{S}_{z1}^2 + \hat{S}_{z2}^2\right) + E\left(\hat{S}_{x1}^2 - \hat{S}_{y1}^2 + \hat{S}_{x2}^2 - \hat{S}_{y2}^2\right) + g\mu_{\mathrm{B}}\mathbf{B}\cdot\left(\hat{\mathbf{S}}_1 + \hat{\mathbf{S}}_2\right)$$

here D and E denote the uniaxial and rhombic single-ion anisotropy parameters, respectively, $\mathbf{S}_i$ is the spin vector at the i-th Ni(II) site (S_i = 1), S_{xi}, S_{yi},and S_{zi} are the projections of $\mathbf{S}_i$ along the x, y, z-directions, **B** is an external magnetic field, μ_B is the Bohr magneton and g is the magnetic g-factor for the Ni(II) ions, assumed to be isotropic. The energy levels were calculated analytically by the diagonalization of the above Hamiltonian's matrix and used to calculate the magnetic properties. The fitting considered the contribution of the capsule sample holder, determined empirically, and the sample diamagnetic contributions to the susceptibility, calculated using Pascal's constants tables, as well as temperature independent paramagnetism (TIP). These contributions amounted to constant values of the magnetic susceptibility of $60\cdot10^{-6}$ and $430\cdot10^{-6}$ cm^3/mol for **1** and **2**, respectively. The best fits presented in Figure S13 were obtained with the help of a genetic algorithm using the PyGAD library.[15] The results for specific model parameters were confirmed numerically using *clique.*[16] The small maxima at low temperatures could have several origins; small amount of crystalline torquing, the presence of spin-spin

[15] A. F. Gad, *Multimed. Tools. Appl.*, 2023, 1–14

[16] M. Antkowiak, Ł. Kucharski, M. Haglauer, *Lecture Notes Comp. Sci.*, 2020, **12044**, 312–322.

interactions or larger |*E*| values. If a *J* coupling is introduced into the fit, the maxima can be reproduced. However, this parameter is correlated with |*E*|. Considering the uncertainty on the origin of the small maxima, we have preferred to avoid overparameterization by keeping the above Hamiltonian for the fit.

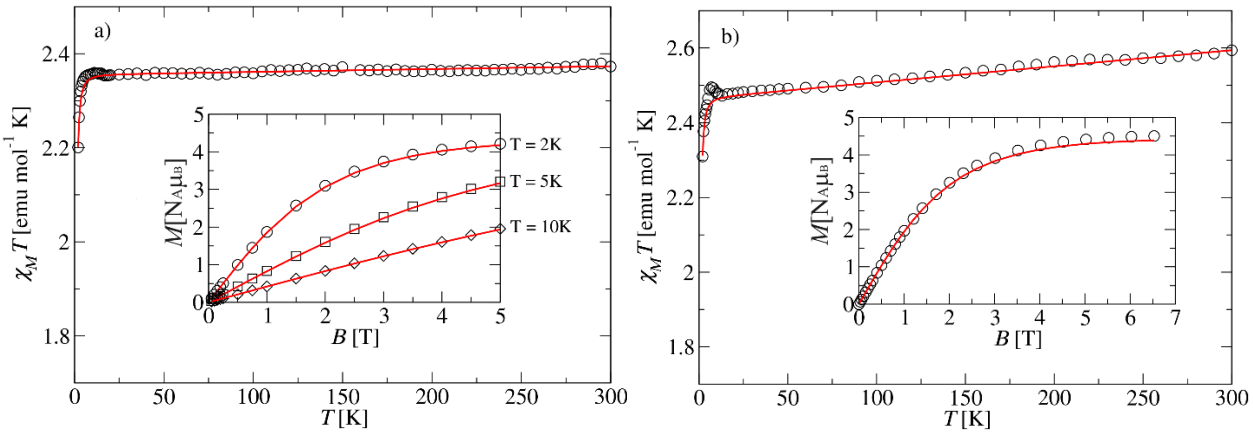

Figure S13. Plots of the temperature dependence of the $\chi_M T$ product for compounds **1** (a) and **2** (b). The insets depict magnetization isotherms measured at T = 2, 5 and 10 K (a) and T = 2 K (b). Symbols represent experimental data and solid lines are best fits (see above text).